Biochemistry

 Volume 35, Number 35 September 3, 1996

Articles

Spin−Lattice Relaxation of the Pheophytin, Pheo$^-$, Radical of Photosystem II[†]

Yiannis Deligiannakis* and A. William Rutherford

Section de Bioénergétique (URA CNRS 2096), Département de Biologie Cellulaire et Moléculaire, CEA Saclay, 91191 Gif-sur-Yvette, France

Received April 9, 1996; Revised Manuscript Received June 24, 1996[⊗]

ABSTRACT: The spin−lattice relaxation times (T_1) of the pheophytin anion radical, Pheo$^-$, of the PSII reaction center, were measured between 5 and 80 K by electron spin-echo spectroscopy. The Pheo$^-$ was studied in Mn-depleted PSII reaction centers in which the primary quinone, Q_A, was doubly reduced. The selective conversion of the non-heme Fe^{2+} into its low-spin ($S = 0$) state, in CN-treated PSII, allowed the measurement of the intrinsic T_1 of the Pheo$^-$ radical. The temperature dependence of the intrinsic $(T_1)^{-1}$ was found to be $\sim T^{1.3\pm0.1}$. In Mn-depleted PSII membranes the high-spin ($S = 2$) non-heme iron, enhances the spin−lattice relaxation of Pheo$^-$. By analyzing the data with a dipolar model, the dipolar interaction (k_{1d}) between the Pheo and the Fe^{2+} ($S = 2$) is estimated over the temperature range 5−80 K. Comparison with the dipolar coupling between the iron and the tyrosine, Y_D^+, shows that the Pheo is much closer to the iron than the Y_D^+ in the PSII reaction center. By scaling the reported $Fe^{2+}-Y_D^+$ distance by the ratio $[k_{1d}\text{Pheo}^-]/[k_{1d}Y_D^+]$, we estimate the $Fe^{2+}-$Pheo$^-$ distance in PSII to be 20 ± 4.2 Å. This distance is close to the $Fe^{2+}-$BPheo$^-$ distance in the bacterial reaction center, and this result provides further evidence that the acceptor sides of the reaction centers in PSII and bacteria are homologous.

In the reaction center of photosystem II (PSII)[1] excitation of the primary electron donor, P_{680}, leads to its oxidation by the primary electron acceptor, Pheo, a pheophytin α molecule (Klimov et al., 1977, 1980). Electron transfer proceeds from Pheo$^-$ to Q_A, a plastoquinone, and then to a second plastoquinone, Q_B. A high-spin non-heme Fe^{2+} ($S = 2$) is situated between the two quinones [for a review on PSII see Hansson and Wydrzynski (1990)].

The midpoint potential of the Pheo$^-$/Pheo couple in PSII, determined by redox titration of the light-induced absorbance changes at 685 nm, is −610 mV (Klimov et al., 1979); this is close to the midpoint potential of the couple Pheo$^-$/Pheo *in vitro* (−640 mV) (Fujita et al., 1978). At ambient redox potentials, photoaccumulation of the Pheo could not be observed; however, under strongly reducing conditions (E_h < −400mV) photoreduction of the Pheo is observed at temperatures from 300 to 5 K (Klimov et al., 1977; Rutherford & Mathis, 1983).

The acceptor side of PSII shares a number of spectroscopic and functional similarities with the bacterial reaction centers [reviewed in Mathis and Rutherford (1987)], and these led to suggestions that the two reaction centers were structurally similar. Amino acid sequence comparisons prompted proposals of folding models for the structure of PSII, based on the crystal structure of the purple bacteria reaction center (Trebst, 1986; Michel & Deisenhofer, 1988). Studies on the

[†] Y.D. was supported by a Human Capital & Mobility Grant, contract ERB0049GI1901. This work was also supported by the H. C. M. Network "MASIMO", contract ERBCHRXCT920072.

* Corresponding author.

[⊗] Abstract published in *Advance ACS Abstracts,* August 1, 1996.

[1] Abbreviations: PSII, photosystem II; Pheo, the pheophytin electron acceptor; Q_A, the primary electron acceptor of the iron−quinone complex; Tyr Y_D^+, tyrosine radical responsible for the continuous wave EPR signal II_{slow}; HEPES, 4-(2-hydroxyethyl)-1-piperazineethanesulfonic acid; MES, 2-(*N*-morpholino)ethanesulfonic acid; Tris, tris(hydroxymethyl)aminomethane; CW EPR, continuous wave electron paramagnetic resonance.

S0006-2960(96)00847-1 CCC: $12.00

electric fields generated by the electron transfer from P_{680} to the Pheo and from Pheo$^-$ to Q_A were interpreted as indicative that the dielectrically weighted distances between P_{680} and Pheo and between Pheo and Q_A are approximately equal (Leibl et al., 1989). Linear dichroism data suggest that the macrocycle plane of Pheo in PSII is perpendicular to the thylakoid membrane plane (Ganago et al., 1982) like in the bacterial reaction center (Deisenhofer et al., 1984; Allen et al., 1988); more recent reports suggest that Pheo is somewhat inclined with respect to the membrane plane (Breton, 1990). Resonance Raman and FTIR studies indicate that, as in the purple bacteria, the 9-keto carbonyl of the Pheo is hydrogen bonded to a glutamic residue (Glu 130 of D1) (Moënne-Loccoz et al., 1989; Naberdryk et al., 1990).

In spite of this amount of information, direct structural information concerning the localization of Pheo in PSII is scarce. EPR studies provide evidence for the proximity of the Pheo to the iron−quinone complex, Q_AFe^{2+} ($S = 2$), at the acceptor side of PSII (Klimov et al., 1980; Zimmermann & Rutherford, 1984). However a recent study of electrochromic shifts in PSII argues for differences in the mutual arrangement of Pheo and Q_A in PSII and their bacterial counterparts (Mulkidjianjan et al., 1996).

The magnetic interaction of the Pheo$^-$ radical with the $Q_A^-Fe^{2+}$ ($S = 2$) complex is a sensitive probe of the magnetic state of the Q_A and the non-heme iron. The state Pheo$^-Q_A^-Fe^{2+}$ ($S = 2$) is characterized by a doublet split signal, assigned to a magnetic interaction between the Pheo$^-$ and $Q_A^-Fe^{2+}$ ($S = 2$) (Klimov et al., 1980; Rutherford & Zimmermann 1984). When the Q_A is doubly reduced, the state Pheo$^-Q_A^{2-}Fe^{2+}$ ($S = 2$) is characterized by an EPR signal with $g = 2.0034$ and $\Delta H = 13$G, characteristic of the Pheo$^-$ anion radical (Klimov et al., 1980; van Mieghem et al., 1989). A similar EPR signal is detected when the non-heme iron is removed from PSII (Klimov et al., 1980).

The study of the magnetic interaction between a radical and a metal can result in useful information like a direct estimation of the interspin distance (Hyde et al., 1979, and references therein). Norris et al. (1980) had shown that in the bacterial reaction center, the non-heme Fe^{2+} ($S = 2$) enhances the spin−lattice relaxation of the $(BChl)_2^+$; more recently several groups have shown that the non-heme Fe^{2+} ($S = 2$) enhances the spin-lattice relaxation of some of the radicals in PSII, i.e., the stable tyrosine radical Y_D^+ (Beck et al., 1990; Evelo & Hoff, 1991; Bosch et al., 1991; Hirsh et al., 1992; Hirsh & Brudvig, 1993; Un et al., 1994; Koulougliotis et al., 1995) the tyrosine radical Y_z^+ (Koulougliotis et al., 1995) a chlorophyll radical Chl_z^+. (Koulougliotis et al., 1994).

In the present work, we report a study of the magnetic interaction between the Pheo$^-$ radical and the non-heme iron in PSII; we have performed measurements of the spin−lattice relaxation of the Pheo$^-$ radical in Mn-depleted PSII at temperatures between 5 and 80 K. We prepared the PSII in two states: in the first the only paramagnetic center in PSII is the Pheo$^-$ radical; the non-heme iron is converted to its low-spin state ($S = 0$) by treating Mn-depleted PSII with CN according to Sanakis et al. (1994). In the second preparation, the PSII contains two paramagnetic species, the Pheo$^-$ radical and the non-heme Fe^{2+} ($S = 2$). In both cases the primary quinone, Q_A, is doubly reduced (Van Mieghem et al., 1989). From the comparative study of the spin−lattice relaxation of Pheo$^-$ with that of the stable tyrosine radical Y_D^+ the Pheo−Fe distance is estimated.

MATERIALS AND METHODS

Sample Preparation. PSII membranes were isolated from market spinach as described previously (Berthold et al., 1981) with the modifications described in Boussac and Rutherford (1988). Mn-depletion was performed by incubating these PSII membranes (0.5 mg of chlorophyll/mL) in 0.8 M Tris-HCl (pH 8.1), 5 mM NaEDTA for 30 min at 0 °C under room light. The Mn-depleted membranes were pelleted and washed once in a buffer containing 60 mM HEPES (pH 8.1), 0.4 M sucrose, 10 mM NaCl, and 5 mM $MgCl_2$ and were resuspended in the same buffer at 4 mg of chl/mL final concentration. In these PSII membranes the non-heme iron was converted to its low-spin state by incubating the Mn-depleted PSII membranes with 350 mM KCN at pH 8.1 for 3 h at 5 °C, according to Sanakis et al. (1994). As a control, Tris-washed PSII membranes were incubated under similar conditions without the KCN. In both types of PSII membranes the Pheo$^-$ radical was induced by a procedure which involved incubation of the membranes under reducing conditions ($E_h = -450 \pm 20$ mV) for 60 min/5 °C, in the dark followed by illumination at 15 °C for 12 min (Van Mieghem et al., 1989). No redox mediator was used. The redox potential was adjusted by sodium dithionite under anaerobic conditions and was measured in the sample with a platinum electrode, with a calomel reference electrode (Russell pH, Auchtermuchty, U.K.) connected to a Tacussel pH/millivolt meter (Tacussel, Villeurbanne, France). Measured redox potentials were normalized to the standard hydrogen electrode, calibrating the electrode using saturated quinhydrone (potential = 286 mV, at pH 6.5). Quantitation of the formation of the Pheo$^-$ radical was done by comparison with the double integral of the CW EPR spectrum of the stable tyrosine radical, Y_D^+, in untreated PSII according to Buser et al. (1992); in CN-treated membranes (pH 8.1) the CW EPR signals detected after illumination were mixtures of the EPR signals of Y_D^+ and Q_A^-. Since at alkaline pH the Y_D^+ radical is not stable (Boussac & Etienne, 1982), we have performed the trapping of the Y_D^+ in CN-treated PSII at pH 6. After the CN treatment, the Mn-depleted PSII membranes were washed and resuspended once in a buffer containing 60 mM MES (pH 6.3), 0.4 M sucrose, 10 mM NaCl, 5 mM $MgCl_2$ followed by illumination at 0 °C for 8 min, dark incubation for 30 s and freezing to liquid nitrogen in the dark; by this protocol we could get CW EPR signals of Y_D^+ with approximately 10% Q_A^-. The contribution of Q_A^- to the spectrum was identified by its characteristic ESEEM spectrum (Deligiannakis et al., 1995); quantitative estimation was made by comparison with the CW EPR spectrum of the Q_A^- generated in CN-treated PSII membranes. The sample used in the present work for the measurements on Y_D^+ in CN-treated PSII membranes contained ~10% of Q_A^-.

Continuous-wave (CW) EPR spectra were recorded at liquid helium temperatures with a Bruker ER 200D X-band spectrometer equipped with an Oxford Instruments cryostat. The microwave frequency and the magnetic field were measured with a microwave frequency counter HP 5350B and a Bruker ER035M NMR gaussmeter, respectively.

Spin−lattice relaxation times, T_1, were measured by saturation recovery at 9.6 GHz on a Bruker ESP 380 spectrometer

with a dielectric resonator, described in Deligiannakis et al. (1995). The saturation recovery was monitored by recording the two-pulse echo intensity ($\pi/2 - 120$ ns $- \pi$; with $t_{\pi/2} =$ 16 ns) as a function of the time after a saturating pulse sequence. The magnetic field corresponded to the maximum intensity of field swept spectrum; in the case of the Y_D^+ in CN-treated PSII membranes the field was shifted plus 5 Gauss from the maximum intensity value, in order to minimize contributions from the Q_A^- to the detected echo. To minimize contributions from spectral diffusion a burst of N saturating pulses was employed (Dalton et al., 1972; Beck et al., 1991). The pulse length was $t_p = 8$ ns corresponding to $H \approx 10$G; typically $N = 30-80$ pulses with an interpulse delay of 0.5−3.0 μs were used. The repetition rate was adjusted in every measurement in order to ensure complete magnetization recovery.

Analysis of the Relaxation Times. The relaxation enhancement of a slowly relaxing spin by a fast relaxing spin was described by Bloembergen (1949) and for a pairwise point−dipole interaction between two isotropic spins with T_{1f}, $T_{2f} \ll T_{1s}$ can be expressed as (Abragam, 1961; Kulikov & Likhtenstein, 1977)

$$k_{1\theta} = \frac{\gamma_s^2 \mu_f^2}{r^6}\left\{ {}^1/_6 \underbrace{\frac{T_{2f}}{1+(\omega_s-\omega_f)^2 T_{2f}^2}(1-3\cos^2\theta)^2}_{B\text{ term}} + 3\underbrace{\frac{T_{1f}}{1+\omega_s^2 T_{1f}^2}\sin^2\theta\cos^2\theta}_{C\text{ term}} + {}^3/_2 \underbrace{\frac{T_{2f}}{1+(\omega_s+\omega_f)^2 T_{2f}^2}\sin^4\theta}_{E\text{ term}} \right\} \quad (1)$$

where f and s denote the fast and slow relaxing spins, respectively; γ_s is the magnetogyric ratio of the slowly relaxing spin, r is the interspin distance, ω_f and ω_s are the resonant frequencies, and θ is the angle between the interspin vector and the external magnetic field. The observed spin−lattice relaxation rate is $k_1 = k_{1i} + k_{1\theta}$ where $k_{1i} = 1/T_{1i}$ and is the intrinsic spin−lattice relaxation rate of the slowly relaxing spin. The recovery trace is described by the equation (Hyde et al., 1979; Hirsh et al., 1992)

$$f(t) = 1 - N\int_0^{\pi} \sin\theta\, e^{-k_1 t}\, d\theta$$

where N is a scaling factor.

For the estimation of the interaction distance from the dipolar enhancement a knowledge of the spin−lattice relaxation times of the fast relaxing spin, in our case the non-heme Fe^{2+} ($S = 2$), enters the problem. The relaxation times of the non-heme iron in PSII have not been directly measured; indirect information comes from the relaxation enhancement of organic radicals in PSII (i.e., Y_D^+, Y_z^+, Chl_z^+) [Koulougliotis et al., 1994, 1995; see also Evelo and Hoff (1991)] by the non-heme Fe^{2+} ($S = 2$) and for the case of radicals in the bacterial reaction center (Norris et al., 1980; Hirsh & Brudvig, 1993). These data in combination with direct spin lattice relaxation measurements of the $Q_A^-Fe^{2+}$ ($S = 2$) complex in the bacterial reaction center at $T < 4$ K (Calvo et al. 1982) provide evidence that in the present case, i.e., microwave frequency 9.6 GHz and temperatures below 80 K, T_{1f} is $>10^{-11}$ s [NB: it is assumed that the T_1 of the Fe is comparable in bacterial reaction centers and in PSII; this seems justified since Mossbauer studies have shown that the crystal field parameters are similar for the iron in both cases (Boso et al., 1981; Petrouleas & Diner, 1982)]. To make the problem tractable we have fitted our experimental data by using separately the B or the C term of eq 1, in the form $k_{1\theta} = k_{1d}(1 - 3\cos^2\theta)^2$ or $k_{1d}\sin^2\theta\cos^2\theta$ respectively, with k_{1d} as the adjustable parameter.

RESULTS

After strong illumination under strongly reducing conditions ($E_h = -450$ mV) the primary quinone is doubly reduced and probably protonated (Q_AH_2) while the pheophytin is singly reduced (Van Mieghem et al., 1989). The CW EPR signal recorded in Mn-depleted PSII membranes with the Q_A doubly reduced in this way is displayed in Figure 1A (solid line); the spectrum consists of a structureless derivative with $\Delta H_{pp} = 13.0 \pm 0.5$G and $g = 2.0034 \pm 0.0003$, i.e., the EPR characteristics of the Pheo$^-$ radical (Klimov et al., 1980). No split EPR signal, indicative of the state $Pheo^-Q_A^-Fe^{2+}$ ($S = 2$), is detected in this sample (data not shown); this indicates that all the detected Pheo$^-$ signal arise from PSII centers in the state $Pheo^-\ Q_A^{2-}Fe^{2+}$ ($S = 2$). Thus, under these conditions the only paramagnetic species expected to be in the Mn-depleted PSII are the Pheo$^-$ radical and the non-heme Fe^{2+} ($S = 2$). Since the membranes are poised under strongly reducing conditions all the stable cationic paramagnetic centers of PSII (Y_D^+, Cyt_{b559}) are reduced.

PSII membranes were treated with CN in order to generate the low-spin ($S = 0$) form of the Fe^{2+} (Sanakis et al., 1994). The efficacy of this treatment was verified by the complete absence of the $Q_A^-Fe^{2+}$ ($S = 2$) EPR signal and the presence of the Q_A^- signal at $g = 2.0045$ in >90% of the centers [see Sanakis et al. (1994) and Deligiannakis et al. (1995)]. In such samples, generation of the Pheo$^-$ radical was done as described above and the spectrum is shown in Figure 1A (dotted line). The signal has the characteristics of the Pheo$^-$ radical. This shows that the CN treatment does not impair the electron donation to Pheo$^-$. In this sample the Pheo$^-$ radical is the only paramagnetic center present since the iron is in the low-spin ($S = 0$) state.

Comparison of the two spectra in 1A shows that under non-saturating conditions there is no resolvable difference in the two EPR spectra. Both spectra consist of a structureless derivative with $\Delta H_{pp} = 13.0$ G and $g = 2.0034$. We have carefully examined the line width as a function of the temperature at non-saturating conditions and within the experimental accuracy of our measurements no difference in the line width of the CW EPR spectrum is resolved in the temperature range $10 < T < 80$ K. Thus the spin state of the non-heme iron has no effect on the CW EPR line shape of the Pheo$^-$. However, a study of the progressive microwave saturation properties of the Pheo$^-$ radicals, revealed a marked relaxation enhancement attributed to the high-spin Fe^{2+}. This effect is shown in Figure 1B; at 30 K the $Pheo^-Fe^{2+}$ ($S = 0$) is saturated at lower microwave powers than the Pheo$^-$ in the presence of the high spin iron. From Figure 1B it is seen that $P_{1/2} = 89$ μW and 690 μW for $Pheo^-Fe^{2+}$ ($S = 0$) and $Pheo^-Fe^{2+}$ ($S = 2$), respectively.

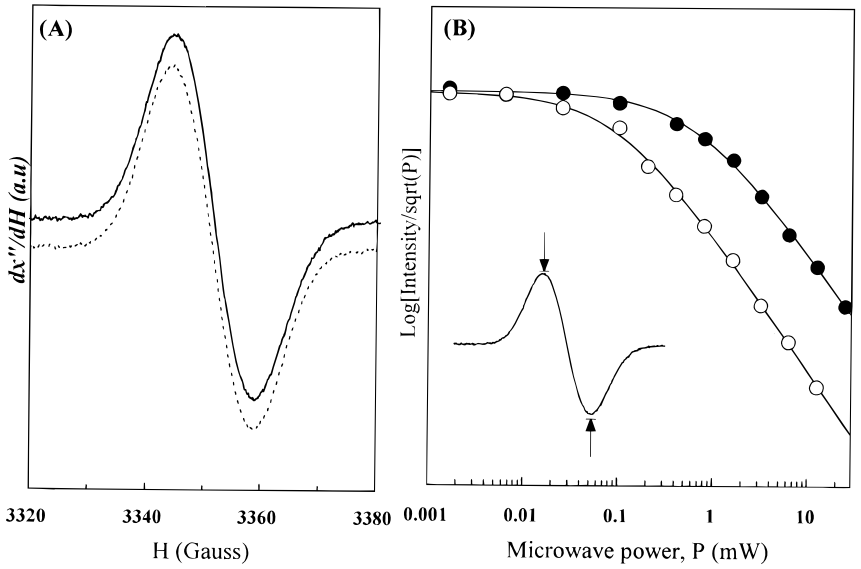

FIGURE 1: (A) CW X-band EPR spectra of Mn-depleted PSII membranes (5 mg of chl/mL, pH 8.1) poised at $E_h = -450$ mV for 60 min followed by illumination at 15 °C for 12 min: CN-treated PSII, $Pheo^-Q_A^{2-}Fe^{2+}$ ($S = 0$) state (dotted line) and $Pheo^-Q_A^{2-}Fe^{2+}$ ($S = 2$) state (solid line). Experimental conditions: temperature, 30 K; microwave frequency, 9.42 GHz; microwave power 200 nW; modulation frequency 12.5 kHz; modulation amplitude, 2 Gauss. (B) Progressive saturation of the intensity of the first-derivative EPR signal of the $Pheo^-Q_A^{2-}Fe^{2+}$ ($S = 2$) (filled circles) and $Pheo^-Q_A^{2-}Fe^{2+}$ ($S = 0$) (open circles). The continuous lines are fits using the equation $I = (1 + P/P_{1/2})^b$ where P is the microwave power; for parameter values see text.

To obtain quantitative information concerning this relaxation enhancement a pulsed EPR study was performed which is presented below. In the case of weak magnetic coupling between the iron and the $Pheo^-$, fast modulation of the interaction, due for example to the fast T_1 of the iron, would result in a more prominent effect on the T_1 than on T_2 of the $Pheo^-$. Indeed two-pulse electron spin echo data on the $Pheo^-$ (not shown) are consistent with this idea but because the T_2 data are perturbed by deep modulations and by T_1 effects, they cannot be taken as an unambiguous demonstration of this effect. However, the absence of a detectable lineshape change on the $Pheo^-$ signal measured by cw EPR is a direct indication that the iron has only a negligible effect on the T_2 of the Pheo. Therefore the T_1 of the $Pheo^-$ should be a more sensitive probe of the interaction (Hyde et al., 1979; Eaton & Eaton 1988a). This possibility was examined by measuring the spin−lattice relaxation time for $Pheo^-Fe^{2+}$ ($S = 0$) and $Pheo^-Fe^{2+}$ ($S = 2$).

Spin−Lattice Relaxation of Pheo$^-$

$Pheo^-Fe^{2+}$ ($S = 0$). The echo-detected EPR spectrum of the $Pheo^-$ in CN-treated BBY is shown in Figure 2A. The spin−lattice relaxation of the $Pheo^-$ was measured by monitoring the saturating recovery of the two-pulse echo at the field position corresponding to the maximum absorption. A typical echo-detected saturation recovery curve of $Pheo^-$ in CN-treated PSII at 16 K is shown in Figure 2B. The recovery is well described by a single exponential; the residual from the fit is shown at the bottom of the transient (Figure 2B). The relaxation measurements were extended over the 5−80 K range; the observed spin−lattice relaxation rates were single exponential over this range. The temperature dependence of the spin−lattice relaxation rates determined in this way are shown in Figure 4 (filled squares).

We noticed that in some CN-treated PSII samples a biexponential character was detected in the case were the double reduction of the Q_A was not complete. In this case the detected transient traces for the $Pheo^-$ contained fractional contributions from a second exponential with rates corresponding to those of Q_A^- in CN-treated PSII (Koulougliotis et al., 1994); the presence of singly reduced Q_A was verified by the characteristic ESEEM pattern (Deligiannakis et al., 1995). We have carefully verified that in the samples used for the data presented in this paper, all of the Q_A was doubly reduced and therefore the $Pheo^-$ is the only radical present.

$Pheo^-Fe^{2+}$ ($S = 2$). A typical echo-detected saturation recovery of the $Pheo^-Fe^{2+}$ ($S = 2$) recorded in Mn-depleted PSII at 17 K is displayed in Figure 3. The recovery is much faster than in the case of the CN-treated Fe^{2+} ($S = 0$) sample. Also in contrast to the $Pheo^-Fe^{2+}$ ($S = 0$) case, the trace is not a single exponential. We have analyzed the data by using the C term of the dipolar model, eq 1, and the least-squares fit is superimposed on the experimental curve, Figure 3. The dipolar rates estimated by the fit at various temperatures are presented in Figure 4 (open squares).

On the basis of this dipolar enhancement, using eq 1, it should in principle be possible to deduce an interspin, Pheo−Fe, distance. Because the relaxation time of the non-heme iron of PSII is unknown, it is not possible to obtain this distance directly. One approach to overcome this is to compare the dipolar effect of the iron on the $Pheo^-$ with its effect on the Y_D^+ radical, for which the Fe−Y_D^+ distance has already been estimated (Koulougliotis et al., 1995). This approach has been used earlier to estimate the Y_Z^+−Fe (Koulougliotis et al., 1995) and Chl_z^+−Fe (Koulougliotis et al., 1994) distances in PSII.

$Y_D^+Fe^{2+}$ ($S = 0$). We found that the illumination at 0 °C of the CN-treated PSII membranes at pH 8.1 results in an EPR signal which is a mixture of the signal of the Y_D^+ (30−40%) and that of the Q_A^- (60−70%) (data not shown). The Q_A^- was identified by its ESEEM pattern (Deligiannakis et al., 1995). The EPR signal of the Y_D^+ generated in the PSII membranes poised at pH 6 after CN treatment, is shown in

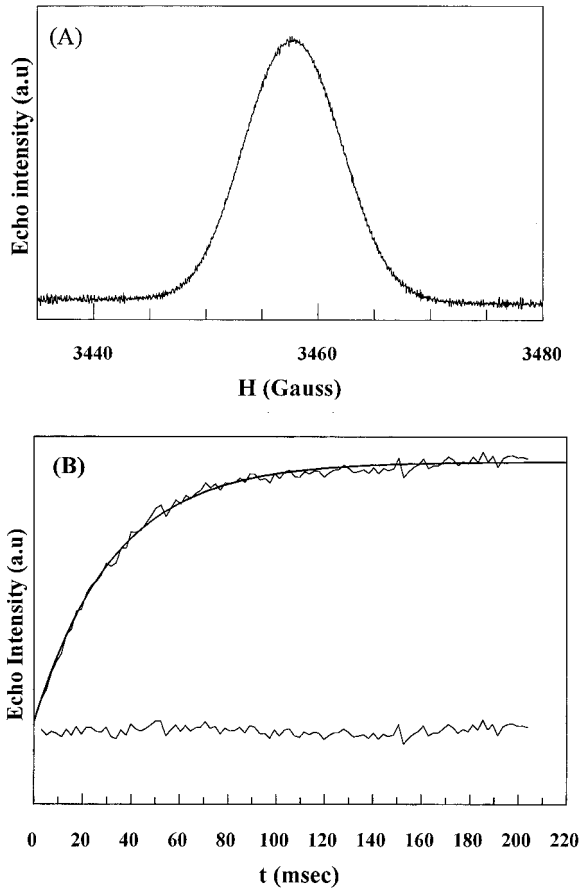

FIGURE 2: (A) Amplitude of the electron spin echo of Pheo⁻ in CN-treated PSII, resulting from a two-pulse sequence ($\pi/2$ − 144 ns − π, with $t_{\pi/2}$ = 16 ns), as a function of the magnetic field. Experimental conditions: sample temperature, 35 K; time interval between successive pulse sets, 5 ms; microwave frequency, 9.6 GHz. (B) Saturation-recovery transient observed for the Pheo⁻ in Mn-depleted PSII treated with CN with the exponential fit superimposed; the difference between the experimental and the fitted curve is shown at the bottom. The two-pulse echo intensity ($\pi/2$ − 120 ns − π, with $t_{\pi/2}$ = 24 ns), was recorded after a sequence of 80 saturating pulses with interpulse separation of 2.6 μs. Experimental conditions: Sample temperature, 16 K; magnetic field strength, 3457 Gauss; two-pulse repetition time, 480 ms; microwave frequency, 9.69 GHz.

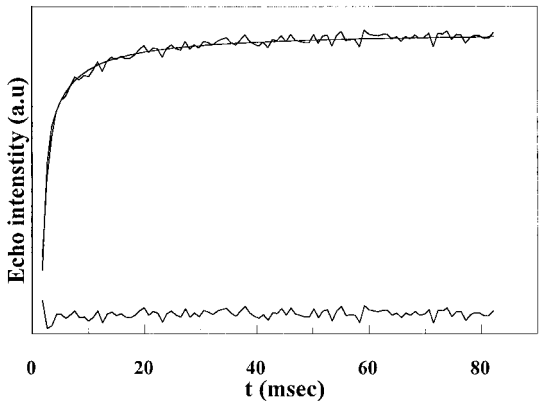

FIGURE 3: Saturation-recovery transient observed for the Pheo⁻ in Mn-depleted PSII. The fit by using the *C* term of eq 1 is superimposed; the difference between the experimental and the fitted curve is shown at the bottom. Experimental conditions: sample temperature, 17 K; magnetic field, 3460 Gauss; two-pulse repetition time, 220 ms; other conditions as in Figure 2B.

Figure 5A (inset). The amplitude of the signal of the Q_A^- in the center of the spectrum part is ∼10% of the Y_D^+ signal.

It is known that in Tris-treated PSII membranes, the Y_D^+ is less stable at pH 8 than at pH 6 (Boussac & Etienne, 1982); this also seems to be the case in CN-treated PSII. For the relaxation measurements the magnetic field was set at plus-5 Gauss from the field corresponding to the maximum absorption signal of the Y_D^+, where the contribution of the Q_A^- is minimal.

A representative saturation recovery trace of the $Y_D^+Fe^{2+}$ (S = 0) at 16 K is displayed in Figure 5A; the temperature dependence of the intrinsic spin−lattice relaxation rate $1/T_{1i}$ determined by a single exponential fit is shown in Figure 4 (filled circles).

$Y_D^+Fe^{2+}$ (S = 2). Figure 4 (open circles) shows the dipolar enhancement of the relaxation rates of Y_D^+ in Mn-depleted PSII when the iron is in the high-spin (S = 2) state. The dipolar rates were estimated by fitting the experimental transients using the *C* term of eq 1; a typical saturation recovery transient is shown in Figure 5B. The data are comparable to those of Koulougliotis et al. (1995) and show the marked relaxation enhancement effect of the iron on the Y_D^+.

When the iron is in the low-spin form, the Pheo⁻ radical relaxes more slowly that the Y_D^+ radical (Figure 4); for example at 30 K the T_{1i} of the Pheo⁻ is ∼ 10 times slower than the T_{1i} of the Y_D^+. At lower temperatures the difference is less pronounced while as the temperature increases the spin−lattice relaxation rates of Y_D^+ and Pheo⁻ diverge. From Figure 4 it is seen that the temperature dependence of the $1/T_{1i}$ of the Pheo⁻ ($\sim T^{1.3}$) is different from that of the Y_D^+ [$\sim T^{2.3}$; see also Koulougliotis et al. (1995)].

Location of the Pheo⁻. The dipolar rates for the Pheo⁻Fe^{2+} (S = 2) are about 2 orders of magnitude higher than for the $Y_D^+Fe^{2+}$ (S = 2). Assuming that the spin−lattice relaxation time of the iron is the same under both experimental conditions (see discussion), then the data indicate that the Pheo⁻−Fe^{2+} distance in PSII is much shorter than the Y_D^+−Fe^{2+} distance. Having estimated the dipolar spin−lattice relaxation enhancement of the Pheo⁻, eq 1 can be used for the estimation of the interspin distance if the T_{1f} of the fast relaxing spin is known. However the T_{1f} for non-heme Fe^{2+} (S = 2) which is the source of the dipolar relaxation enhancement of the Pheo⁻, has not been measured. Nevertheless, an estimate of the Fe^{2+}−Pheo⁻ distance can be made based on the reported Fe^{2+}−Y_D^+ distance. From the values of k_{1d} which are estimated using the *C* term of eq 1, the ratio $R_{Fe-Pheo}/R_{Fe-Y_D}$ is 0.54 ± 0.08; if we consider that the distance R_{Fe-Y_D} is ∼37 Å (Koulougliotis et al., 1995), then $R_{Fe-Pheo}$ = 20 ± 3 Å.

The dipolar rates shown in Figure 3 have been extracted by using the *C* term of eq 1. We have analyzed the experimental data by using the *B* term also; the dipolar rates estimated in this way were about 3−5 times slower than those shown in Figure 4 for both the Pheo⁻ and the Y_D^+. Since the estimate Pheo−Fe distance is based on the ratio of the dipolar rates for the Y_D^+ and the Pheo⁻, the distance obtained by using the *C* or the *B* term is the same.

DISCUSSION

We have studied the Pheo⁻ anion radical in Mn-depleted PSII membranes with the Q_A doubly reduced, in which the non-heme iron was in either the high-spin Fe^{2+} (S = 2) state or in the CN-treated low-spin Fe^{2+} (S = 0) state. For

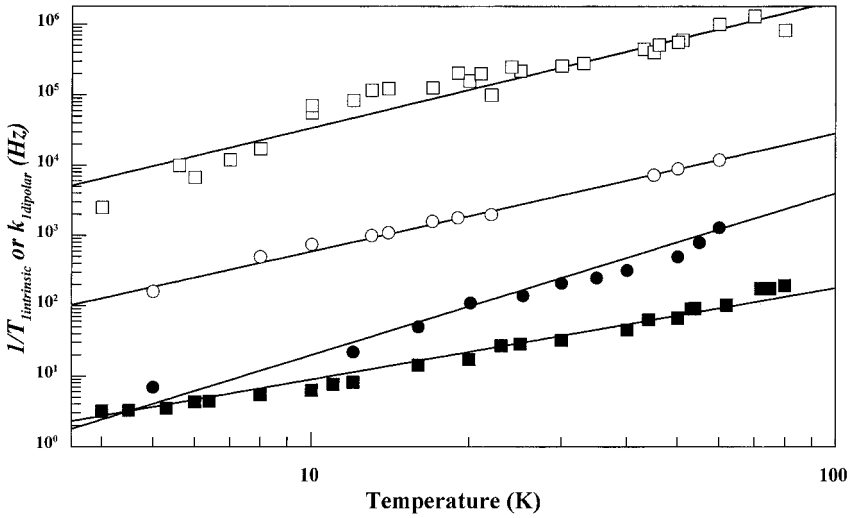

FIGURE 4: Filled symbols: temperature dependence of the intrinsic spin−lattice relaxation rate ($1/T_{1i}$) for Pheo$^-$ (filled squares) and Y_D^+ (filled circles) in Mn-depleted PSII membranes treated with CN. Open symbols: temperature dependence of the dipolar enhancement rates k_{1d} for the Pheo (open squares) and Y_D^+ (open circles) in Mn-depleted PSII membranes, estimated by using the C term of eq 1. The solid lines show power-low (i.e., $1/T_{1i}$ or $k_d \approx T^\eta$ where T is the temperature) fits for each set of the rates: Pheo$^-$Fe^{2+} ($S = 0$) ($1/T_{1i} \approx 0.32T^{1.3\pm0.1}$), Y_D^+Fe^{2+} ($S = 0$) ($1/T_{1i} \approx 0.13T^{2.3\pm0.1}$) and Pheo$^-$Fe^{2+} ($S = 2$) ($k_{d1} \approx 540T^{1.8\pm0.2}$), Y_D^+Fe^{2+} ($S = 2$) ($k_{d1} \approx 12.6T^{1.7\pm0.1}$).

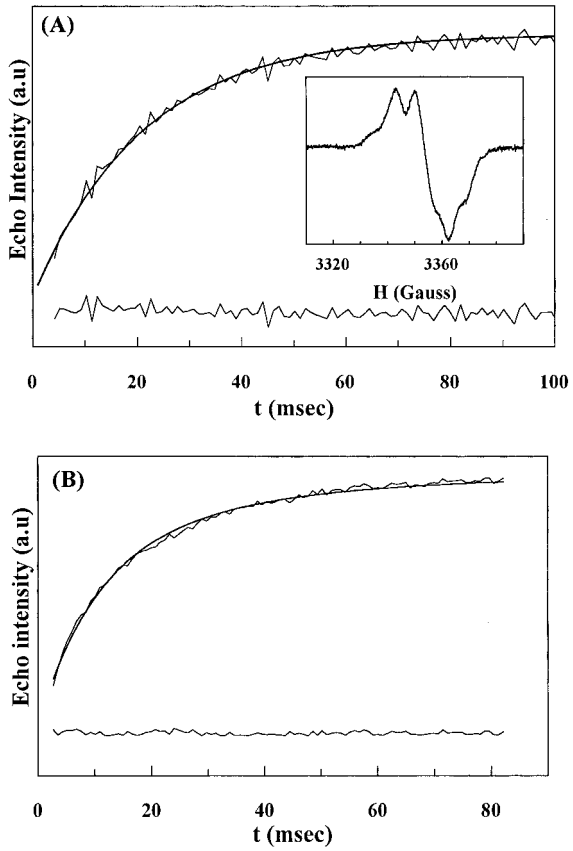

FIGURE 5: (A) Saturation-recovery transient observed for the Y_D^+ in Mn-depleted PSII treated with CN (i.e., Fe^{2+} ($S = 0$)). The exponential fit is superimposed; the difference between the experimental and the fitted curve is shown at the bottom. Inset: CW EPR spectrum at 22 K. (B) Saturation recovery transient observed for the Y_D^+ in Mn-depleted PSII (i.e., Fe^{2+} ($S = 2$)). The fit by using the C term of eq 1 is superimposed; the difference between the experimental and the fitted curve is shown at the bottom. Experimental conditions: sample temperature, 17 K (A) and 16 K (B); magnetic field, 3464 Gauss; microwave frequency, 9.65 GHz; other experimental conditions as in Figures 3 and 2B, respectively.

comparison we have performed the same measurements on the Y_D^+ radical in Mn-depleted PSII with the iron in the high- and low-spin state. No static effect, i.e., line shape change in Pheo$^-$, due to its interaction with the non-heme iron of PSII was detected by CW EPR. However the interaction with the rapidly relaxing Fe^{2+} ($S = 2$) center decreases the spin-lattice relaxation time of the Pheo$^-$. A quantitative estimation of the dipolar interaction between the two paramagnetic centers provides an estimate of the distance between the pheophytin and the iron, $R_{Fe-Pheo} = 20 \pm 3$ Å.

Location of Pheo in PSII. The Fe^{2+}−Pheo distance estimation, taken as an average center-to-center distance, is based on the point-dipole approximation for the description of the magnetic interaction between the pheophytin and the iron. The spin density of the pheophytin anion is distributed over the macrocycle of the molecule; taking into account the dimensions of the pheophytin macrocycle, this would also introduce an average uncertainty of ∼3 Å in the estimated Pheo−Fe distance. This error from the point dipole approximation taken with that due to the T_1 determination results in a combined error of 4.2 Å.

It is of relevance to compare this distance with the homologous distance from the crystal structure of the bacterial reaction centers. The homologous distance in the reaction center is 18.1 Å in *Rhodopseudomonas viridis* (Deisenhofer & Michel, 1984) and 18.4 Å in *Rhodobacter sphaeroides* (Ermler et al.; 1994). Thus the value estimated here for PSII is, within the experimental error, similar to that in the bacterial reaction center. Models of the PSII reaction center have frequently taken the positions of the electron acceptor side components as being virtually the same as those in the bacterial reaction center [e.g., Mathis and Rutherford (1987) and Svensson (1995)]. This is supported by indications from spectroscopic studies. For the pheophytin, its magnetic interaction with the Q_A^-Fe^{2+} ($S = 2$) (Klimov et al., 1980; Rutherford & Zimmermann, 1984) its ring orientation (Ganago et al., 1982) and interactions with homologous aminoacids (Moënne-Loccoz et al., 1989; Naberdryk et al., 1990) provided support for this view. The present data provide direct evidence in support of such models.

The validity of the distance measurement depends on the assumption that the Fe^{2+} ($S = 2$) is in a comparable position and environment under the conditions used to measure the magnetic interaction for Y_{D+}−Fe^{2+} and Pheo$^-$−Fe^{2+}. Recent Mossbauer and EPR data have shown that the crystal field of the iron in PSII is not affected by double reduction of the Q_A (Vass et al., 1994). The temperature dependence of the dipolar rate is a characteristic of the fast relaxing spin; in the case of the Pheo$^-$ in PSII the observed dipolar rate is $\sim T^{1.8\pm0.2}$ while in the case of Y_D^+ it is $\sim T^{1.7\pm0.1}$. The latter is similar to that reported by Koulougliotis et al. (1995, and references therein). The similar temperature dependence is indicative that the environment of the iron in PSII membranes from spinach is comparable in the two cases. It therefore seems likely that the Fe^{2+} ($S = 2$) is unaltered by the treatments given in this work and thus the distance estimate is reliable.

Recently, based on elecrochromic difference spectroscopy it has been suggested that the pigments of PSII, including the Q_A and the Pheo, occupy positions which differ significantly from their arrangement in the bacterial reaction center (Mulkidjanian et al., 1996). In contrast, the present data indicate that the Fe−Pheo distance is rather similar in the bacteria and PSII.

Intrinsic Relaxation of Pheo$^-$. The measured intrinsic spin−lattice relaxation of the Pheo$^-$ is slower than that of the plastoquinone radical Q_A^- and the tyrosine radicals Y_D^+ and Y_z^+ (Koulougliotis et al., 1995) of PSII. On the other hand the intinsic relaxation rate of the Pheo$^-$ is rather similar in magnitude and temperature dependence to that reported for the Chl_z^+ radical in PSII (Koulougliotis et al. 1994). A temperature dependence of $\sim T^1$ has been observed in other radicals in photosynthetic systems like $(BChla)^+_2$ in *Rb. sphaeroides* (Hirsh & Brudvig, 1993) and $Chla_z^+$ in PSII treated with CN (Koulougliotis et al., 1995). Since the pheophytin resonance line is broadened by hyperfine interaction (Fujita & Davis, 1978), we consider that the dominant spin−lattice relaxation mechanism is modulation of the hyperfine interaction by the lattice vibrations [for a review see Bowman and Kevan (1979) and references therein]. Various possible mechanisms can result in a T^1 dependence of the spin−lattice relaxation: (a) a direct (one-phonon) process; however it is unlikely that such a process would be dominant at temperatures higher than a few degrees K. (b) The modulation of the electron nuclear interaction by tunneling of nuclei or molecular groups in the environment of the radicals or local vibrations has been observed in other systems (Murphy, 1966; Bowman & Kevan, 1979, and references therein). Interestingly, a highly rigid environment was suggested to be correlated with the observed $\sim T^1$ temperature dependence for the aforementioned radicals in bacteria and PSII (Koulougliotis et al., 1994; Hirsh & Brudvig, 1993). The estimated Fe−Phe distance, taking into account the structure of the bacterial reaction center, is indicative for the location of the Pheo at the center of the PSII reaction center. In this context the location of the Pheo$^-$ in a highly rigid environment could be anticipated in accordance with the observation based on the temperature dependence of the intrinsic relaxation.

Exchange Interaction. Empirical correlations of the form $J(R) \approx \exp(-bR)$ have been suggested for the relation between the isotropic exchange interaction J and the interspin distance R [see Eaton and Eaton (1988a,b) and references therein]. Moser and Dutton (1992), on the basis of electron transport data, have suggested $b = 1.7$ Å^{-1} (J in Gauss). According to this formula, for a distance of $R \approx 18$ Å, the isotropic exchange interaction is $J < 1$ kHz. The anisotropic exchange interaction is expected to be of the order of the isotropic exchange scaled by the g-anisotropy (Moriya, 1963). Thus the anisotropic exchange interaction between the pheophytin and the iron in PSII, is expected to be negligible; this is in agreement with analogous reports on the bacterial reaction center (Van der Brink et al., 1996).

The effect of an isotropic exchange interaction on the scalar T_1 of the Pheo$^-$ would be $\sim JT_{2f}/(1 + (\omega_s - \omega_f)^2T_{2f}^2)$ (Abragam, 1961) and its contribution would be detected as a faster scalar rate for Pheo. In the present case the scalar rates of the Pheo$^-$$Fe^{2+}$ ($S = 2$), estimated from the fit to the experimental data, are similar to the intrinsic rates of the Pheo$^-$ (data not shown).

A possible exchange interaction would modify the spin density distribution on the macrocycle of the Pheo radical. We have performed ESEEM and ENDOR experiments on the Pheo in the presence of the high-spin and the low-spin iron; the detected hyperfine couplings of the protons and of the nitrogens of the tetrapyroles appear identical in the two cases (Deligiannakis, MacMillan, and Rutherford, manuscript in preparation). According to these data, the magnetic interaction with the iron does not measurably modify the spin density on the macrocycle of the Pheo. We can conclude that spin density modifications on the Pheo radical which might exist due to exchange coupling to the iron are below the resolution of the technique. Given that the accuracy of ESEEM, these data indicate that the exchange interaction, if present, is smaller than 50 kHz this result is consistent with the exchange interaction expected based on the Pheo−Fe distance (i.e., $J < 1$ kHz).

In applying the dipolar model for the description of the interaction between the iron and the Pheo$^-$ we have supposed that the dipolar coupling is the only source of the observed distribution of the relaxation times. Given the arguments considered above, this supposition seems justified.

The EPR signal of the state Pheo$^-$$Q_A^-$$Fe^{2+}$ ($S = 2$) at $T < 10$ K is a doublet signal (Klimov et al., 1980) with an apparent dependence on the pH (42 G at pH 6, 50 G at pH 8) (Rutherford & Zimmermann, 1984). An analogous split signal is detected in the reaction center of *Chlorobium vinosum* or *R. viridis* but not in *R. sphaeroides* [Dutton et al., 1978; Okamura et al., 1979; see also van der Brink et al. (1996)]. This type of split signals has been reported in other systems [see Eaton and Eaton (1988a,b)]. The present data show that in PSII, after double reduction of the Q_A, the interaction between the Pheo$^-$ and the non-heme iron is weak. This is in striking contrast to the ∼60 Gauss (∼200 MHz) splitting detected in the state Pheo$^-$$Q_A^-$$Fe^{2+}$ ($S = 2$). The observed modification of the Fe−Pheo interaction after double reduction of the Q_A could be due to a modification of the exchange or the dipolar coupling or both. It is clear that the presence of the semiquinone, which is magnetically coupled to the iron and situated between Fe and Pheo, greatly influences the distance, and therefore the dipolar coupling, between the interacting spin systems. The presence of Q_A^- could also affect the orbital overlap, direct or indirect, between the Fe and the Pheo and thus have an important effect on the exchange interaction.

It is tempting to consider that the orbitals of Q_A form part of an exchange pathway between the Pheo and the iron. We have attempted to study by electron spin echo spectroscopy the $Pheo^-$ in PSII membranes in the state $Pheo^-Q_A^-Fe^{2+}$ ($S = 2$); however, even at 4 K no echo is detected indicating that the phase memory time or the spin−lattice relaxation time of the Pheo is <200 ns under these conditions. This shows that the interaction between the Pheo and the iron is very different in the presence of Q_A^- compared to Q_A^{2-}. This suggests that the orbitals of the quinone play a crucial role in determining the magnetic coupling between the Pheo and the iron. In this regard it would be interesting to study the interaction between the Q_A^- and the $Pheo^-$ in the absence of the paramagnetic iron.

ACKNOWLEDGMENT

We appreciate stimulating discussions with A. Boussac and S. Un.

REFERENCES

Abragam, A. (1961) *The Principles of Nuclear Magnetism*, Clarendon Press, Oxford.

Beck, W. F., Innes, J. B., & Brudvig, G. W. (1990) in *Current Research in Photosynthesis* (Baltscheffsky, M., Ed.) p 817, Kluwer Academic Publishers, Dordrecht, The Netherlands.

Berthold, D. A., Babcock, G. T., & Yocum, C. F. (1981) *FEBS Lett. 134*, 231.

Bloembergen, N. (1949) *Physica 15*, 386.

Bosch, M. K., Evelo, R. G., Styring, S., Rutherford, A. W., & Hoff, A. J. (1991) *FEBS Lett. 292*, 279−283.

Boso, J., Debrunner, P., Okamura, M. Y., & Feher, G. (1981) *Biochim. Biophys. Acta 638*, 173.

Boussac, A., & Etienne, A.-L. (1982) *FEBS Lett. 148*, 15.

Boussac, A., & Rutherford, A. W. (1988) *Biochemistry 27*, 3476.

Bowman, M. K., & Kevan, L. (1979) in *Time Domain Electron Spin Resonance* (Kevan, L., & Schwartz, R. N., Eds.) p 67, Wiley-Interscience, New York.

Breton, J. (1990) in *Perspectives in Photosynthesis* (Jortner, J., & Pullman, B., Eds.) pp 23−38, Kluwer Academic Publishers, Dordrecht, The Netherlands.

Buser, C. A., Diner, B. A., & Brudvig, G. W. (1992) *Biochemistry 31*, 11441.

Calvo, R., Butler, W. F., Isaacson, R. A., Okamura, M. Y., Fredkin, D. R., & Feher, G. (1982) *Biophys. J. 37*, 111a.

Dalton, L. R., Kwiram, A. L., & Cowen, L. A. (1972) *Chem. Phys. Lett. 17*, 495.

Deisenhofer, J., Epp, O., Miki, K., Huber, R., & Michel, H. (1984) *J. Mol. Biol. 180*, 385.

Deligiannakis, Y., Boussac, A., & Rutherford, A. W. (1995) *Biochemistry 34*, 16030.

Dutton, P. L., Prince, R. C., & Tiede, D. M. (1978) *Photochem. Photobiol. 28*, 939.

Eaton, S. S., & Eaton, G. R. (1988a) *Coord. Chem. Rev. 83*, 89.

Eaton, G. R., & Eaton, S. S. (1988b) in *Biological Magnetic Resonance* (Berliner, L. J., & Reuben, J., Ed.) Vol. 8, 339.

Ermler, U., Fritzsch, G., Buchanan, S. K., & Michel, H. (1994) *Curr. Biol. 2*, 925.

Evelo, R. G., & Hoff, A. J. (1991) *J. Magn. Reson. 95*, 495.

Fujita, I., Davis, M. S., & Fajer, J. (1978) *J. Am. Chem. Soc. 100*, 6280.

Ganago, B., Klimov, V. V., Ganago, A. O., Shuvalov, V. A., & Erokhin, Y. E. (1982) *FEBS Lett. 140*, 127.

Hansson, Ö., & Wydrzynski, T. (1990) *Phosynth. Res. 23*, 131.

Hirsh, D. J., & Brudvig, G. W. (1993) *J. Phys. Chem. 97*, 13216.

Hirsh, D. J., Beck, W. F., Innes, J. B., & Brudvig, G. W. (1992) *Biochemistry 31*, 532.

Hyde, J. S., Swartz, H. M., & Antholine, W. E. (1979) in *Spin Labeling II: Theory and Applications* (Berliner, L. J., Ed.) pp 71−113, Academic Press, New York.

Klimov, V. V., Klevanic, A. V., Shuvalov, V. A., & Krasnovsky, A. A. (1977) *FEBS Lett. 82*, 183.

Klimov, V. V., Allekhverdiev, S. I., Demeter, S., & Krasnovsky, A. A. (1979) *Dokl. Akad. Nauk USSR 249*, 227.

Klimov, V. V., Dolan, E., Shaw, E. R., & Ke, B. (1980) *Proc. Nat. Acad. Sci. U.S.A. 77*, 7227.

Komiya, H., Yeates, T. O., Rees, D. C., Allen, J. P., & Feher, G. (1988) *Proc. Nat. Acad. Sci. U.S.A. 85*, 9012.

Koulougliotis, D., Innes, J. B., & Brudvig, G. W. (1994) *Biochemistry 33*, 11814.

Koulougliotis, D., Tang, X.-S., Diner, B. A., & Brudvig, G. W. (1995) *Biochemistry 34*, 2850.

Kulikov, A. V., & Likhtenstein, G. I. (1977) *Adv. Mol. Relax. Interac. Processes 10*, 47.

Leibl, W., Breton, J., Deprez, J., & Trissl, H.-W. (1989) *Photosyn. Res. 22*, 257.

Mathis, P. & Rutherford, A. W. (1987) in *New Comprehensive Biochemistry, Photosynthesis* (Amesz, J., Ed.) Vol. 15, p 63, Elsevier, Amsterdam.

Michel, H., & Deisenhofer, J. (1988) *Biochemistry 27*, 1.

Moënne-Loccoz, P., Robert, B., & Lutz, M. (1989) *Biochemistry 28*, 3641.

Moriya, Y. (1963) in *Magnetism* (Rado, G. T., & Souhl, H., Eds.) Vol. 1, p 85, Academic, New York.

Moser, C. C., & Dutton, P. L. (1992) *Biochim. Biophys. Acta* 1101, 171.

Mulkidjanian, A. Y., Cherepanov, D. A., Haumann, M., & Junge, W. (1996) *Biochemistry 35*, 3093.

Murphy, J. (1966) *Phys. Rev. 145*, 241.

Naberdryk, E., Andrianambinitsoa, S., Berger, G., Leonhard, M., Mäntele, W., & Breton, J. (1990) *Biochim. Biophys. Acta* 1016, 49−54.

Norris, J. R., Thurnauer, M. C., & Bowman, M. K. (1980) *Adv. Biol. Med. Phys. 17*, 365.

Okamura, M. Y., Isaacson, R. A., & Feher, G. (1979) *Biochim. Biophys. Acta 546*, 394.

Petrouleas, V. V., & Diner, B. A. (1982) *FEBS Lett. 147*, 111.

Rutherford, A. W., & Mathis, P. (1983) *FEBS Lett. 154*, 328.

Rutherford, A. W., & Zimmermann, J.-L. (1984) *Biochim. Biophys. Acta 767*, 168.

Sanakis, Y., Petrouleas, V., & Diner, B. A. (1994) *Biochemistry 33*, 9922.

Svensson, B. (1995) Ph.D. Thesis, Department of Biochemistry, University of Stockholm, Stockholm, Sweden.

Trebst, A. (1986) *Z. Naturforsch. 41c*, 240.

Un, S., Brunel, L.-C., Brill, T. M., Zimmermann, J.-L., & Rutherford, A. W. (1994) *Proc. Natl. Acad. Sci. U.S.A. 91*, 5262.

Van der Brink, J. S., Gast, P., & Hoff, A. J. (1996) *J. Chem. Phys. 104*, 1805.

Van Mieghem, F. J. E., Nitschke, W., Mathis, P., & Rutherford, A. W. (1989) *Biochim. Biophys. Acta 977*, 207.

Vass, I., Sanakis, Y., Spetea, C., & Petrouleas, V. (1995) *Biochemistry 34*, 4434.

BI9608471